Available online at www.sciencedirect.com
ScienceDirect
Developmental Biology 308 (2007) 407–420
DEVELOPMENTAL BIOLOGY
www.elsevier.com/developmentalbiology

Tshz1 is required for axial skeleton, soft palate and middle ear development in mice

Nathalie Coré [a,*], Xavier Caubit [a], Aïcha Metchat [a,1], Annie Boned [b], Malek Djabali [b], Laurent Fasano [a]

[a] *Institut de Biologie du Développement de Marseille-Luminy (IBDML), UMR6216, CNRS, Université de la Méditerranée, F-13288 Marseille cedex 09, France*
[b] *Centre d'Immunologie de Marseille-Luminy (CIML), UMR6102/U631, CNRS-INSERM, Université de la Méditerranée, F-13288 Marseille cedex 09, France*

Received for publication 22 January 2007; revised 4 May 2007; accepted 29 May 2007
Available online 4 June 2007

Abstract

Members of the *Tshz* gene family encode putative zinc fingers transcription factors that are broadly expressed during mouse embryogenesis. *Tshz1* is detected from E9.5 in the somites, the spinal cord, the limb buds and the branchial arches. In order to assess the function of *Tshz1* during mouse development, we generated *Tshz1*-deficient mice. *Tshz1* inactivation leads to neonatal lethality and causes multiple developmental defects. In the craniofacial region, loss of *Tshz1* function leads to specific malformations of middle ear components, including the malleus and the tympanic ring. *Tshz1*$^{-/-}$ mice exhibited Hox-like vertebral malformations and homeotic transformations in the cervical and thoracic regions, suggesting that *Tshz1* and *Hox* genes are involved in common pathways to control skeletal morphogenesis. Finally, we demonstrate that *Tshz1* is required for the development of the soft palate.

Keywords: Tshz1; Mouse development; Gene inactivation; Middle ear; Malleus; Axial skeleton patterning; Soft palate; CAA

Introduction

The *Tshz* genes were formerly identified in *Drosophila* as regulators of tissue patterning (Bessa et al., 2002; Erkner et al., 1999; Fasano et al., 1991; Mathies et al., 1994; Pan and Rubin, 1998; Singh et al., 2002). Three *Tshz*-related genes, *Tshz1*, *Tshz2* and *Tshz3*, have been isolated in vertebrates (chick, mouse, human) based on sequence homology. Our recent finding that the murine *Tshz* genes are able to rescue trunk defects in *tsh*-deficient flies demonstrated that they are functional homologs of *Drosophila teashirt* (Manfroid et al., 2004). The structural organization of the Tshz proteins has been well conserved during evolution and the Tshz protein family is characterized by the presence of 3 conserved atypical zinc finger motifs that have been shown to bind DNA in in vitro experiments (Alexandre et al., 1996). Moreover, Tsh behaves as a transcriptional repressor in transfected mammalian cells (Manfroid et al., 2004; Waltzer et al., 2001). In *Drosophila*, several studies have revealed tight but complex regulatory relationships between Tsh and Hox proteins during morphogenesis (de Zulueta et al., 1994; Fasano et al., 1991; Mathies et al., 1994; McCormick et al., 1995; Roder et al., 1992). Like Hox proteins, Tsh displays homeotic functions and it has been shown that *tsh*-loss and gain-of-function mutants exhibit homeotic transformation of segmental identity along the antero-posterior axis of the embryo (de Zulueta et al., 1994; Fasano et al., 1991).

However, the biological function of the *Tshz* genes during mammalian development remains unknown. In mice, the three *Tshz* genes are expressed in several tissues and developing organs during embryogenesis (Caubit et al., 2000). In the body part of the embryo, as well as during forebrain development, *Tshz* genes are expressed in overlapping or exclusive domains (Caubit et al., 2000, 2005). These results suggest that the different *Tshz* genes probably accomplish non-redundant functions during development.

* Corresponding author. Fax: +33 4 91 82 06 82.
E-mail address: ncore@ibdml.univ-mrs.fr (N. Coré).
[1] Present address: Centre de Biologie du Développement, UMR5547, Université Paul Sabatier, F-31062 Toulouse cedex 9, France.

0012-1606/$ - see front matter © 2007 Elsevier Inc. All rights reserved.
doi:10.1016/j.ydbio.2007.05.038

Among members of the *Tshz* family, only *Tshz1* is expressed in neural crest-derived mesenchymal cells of the first and second branchial arches. Tshz1 is also strongly expressed in the somites, along the antero-posterior axis of the embryo, from which the axial skeleton develops. The expression of *Tshz1* in the branchial arches is detected in cell populations that will give rise to components of the middle ear. Skeletal development in the branchial arches requires molecular interactions between the epithelial and the mesenchymal compartments (Santagati and Rijli, 2003). In this context, it has been shown that mesenchymal expression of *Tshz1* during branchial arch development is controlled by signaling molecules from the overlying epithelium and that *Tshz1* behaves as a downstream effector of Fgf8 and Bmp4 signaling (Long et al., 2001). Together these data suggest that *Tshz1* could play a role in developmental processes, including the formation of the axial skeleton and the development of branchial arch derivatives.

In this study, we investigated the function of *Tshz1* during mouse development by generating *Tshz1*-deficient mice. *Tshz1* inactivation leads to neonatal lethality and *Tshz1*$^{-/-}$ newborns exhibit a strong defect of the soft palate. We observed vertebral malformations in the cervical and thoracic regions of the axial skeleton of *Tshz1*-null newborns, reminiscent of phenotypes previously described in *Hox* mutant mice. Finally, analysis of the craniofacial region of *Tshz1*-null mice revealed that *Tshz1* deficiency specifically leads to malformations in the middle ear components. Together, these results demonstrate that *Tshz1* gene is necessary for normal development of specific structures in mouse.

Materials and methods

Gene targeting of the Tshz1 locus

DNA fragments from the *Tshz1* locus were isolated from a 129/Ola mouse genomic library screened by a 0.8 kb *Eco*RI/*Xho*I fragment digested from an EST clone (dbest id: AA589598). For the targeting construct, two fragments flanking exon 2 were sub-cloned into the pBS-neo-loxP vector described elsewhere (Core et al., 1997). The 0.5 kb *Eco*RV/*Xmn*I fragment containing the first 300 bp of exon 2 was fused to an EGFP coding sequence (Clontech Lab.). However, the GFP protein was not properly translated from the targeted allele, due to a mutation that prematurely inserts a stop codon. The 5.5 kb *Bam*HI fragment contained genomic DNA located 3′ to the *Tshz1* transcription unit. The HSV-TK sequence (McKnight, 1980) was cloned into the targeting vector as a negative selection gene. E14 (129/Ola) ES cells were electroporated by 20 μg of recombinant plasmid. Homologous recombinants were tested by hybridization of *Hin*dIII-digested genomic DNA using a *Hin*dIII/*Bam*HI fragment as an external probe. The neomycin sequence was used as a probe to check unique integration event and the 5.5 kb *Bam*HI fragment was used to control for correct recombination 3′ to the locus.

Generation of Tshz1-null mice

Male chimeras were generated after injection of *Tshz1*$^{+/-}$ ES cells into C57BL/6J blastocysts and mated to C57BL/6J females. F1 heterozygous offspring were inter-crossed to obtain homozygous mice for *Tshz1* mutation. Alternatively, F1 heterozygous males were crossed to CD-1 females to generate *Tshz1* mutants on CD-1 genetic background. Genotyping was done by PCR on genomic DNA. Two primers from the neomycine sequence allowed amplification of a 478-bp fragment from the recombinant allele (5′-GGAAGG GACTGGCTGCTATTG-3′ and 5′-CGATACCGTAAAGCACGAGG-3′), two primers from exon 2 allowed amplification of a 190-bp fragment from the wild type allele (5′-GACGAGCTGTCACCTGTTCA-3′ and 5′-GATGGTGGT-CATGGATAGGC-3′). PCR conditions were as follows: 1 cycle at 94 °C for 5 min, 30 cycles at 94 °C for 45 s, 60 °C for 30 s, 72 °C for 45 s.

Skeletal preparations

Whole mount skeletons were stained as described (Core et al., 1997).

Histological analysis and in situ hybridization

Skinned fetuses and newborns were fixed in 4% paraformaldehyde, dehydrated, cleared and embedded in paraplast. Serial sections at 10 μm were stained with hematoxylin/eosin. For cartilage and bone detection, sections were treated successively by the following solutions: 10 min in Weigert hematoxylin, differentiated a few seconds in 70% ethanol/1% HCl, 10 min in 1% Alcian blue 8GX in 1% glacial acetic acid, 10 min in 1% phosphomolybdic acid and then 30 min in 0.5% Sirius red in 30% picric acid.

RNA in situ hybridization on whole mount embryos and sections was performed as described (Henrique et al., 1995; Tiveron et al., 1996). The probes used were *Bapx1* (Lettice et al., 2001), *Cbfa1* (Ducy et al., 1997), *Dlx3* (Morasso et al., 1996), *GFP* (a gift from F. Watrin), *Gsc* (Gaunt et al., 1993), *Hoxa2* (Hunt et al., 1991), *Hoxa3* (Gaunt, 1987), *Hoxd4* (Bel-Vialar et al., 2000), *Hoxc8* (Bel et al., 1998), *Lhx6* (Grigoriou et al., 1998), *Msx1* (Robert et al., 1989), *Sall3* (Ott et al., 1996), *Sox9* (Morais da Silva et al., 1996) and *Tshz1* (Caubit et al., 2000).

Results

Targeted inactivation of Tshz1 gene

The mouse *Tshz1* locus is composed of 2 exons separated by a 69-kb-long intron, the first exon encoding only 13 amino acids of the protein. In order to inactivate *Tshz1*, we deleted most of exon 2 that encodes 1068 amino acids, including the zinc finger motifs (Fig. 1A). Heterozygous animals were viable, fertile and undistinguishable from the wild type littermates. Heterozygous males and females were inter-crossed to generated homozygous progeny. Litters were genotyped by PCR as illustrated in Fig. 1C. Although the GFP reporter gene introduced in the targeting construct fails to produce fluorescent protein (see Materials and methods), we were able to detect *Tshz1-GFP* fusion transcripts by in situ hybridization using a *GFP* riboprobe. As shown in Fig. 1D, the expression pattern of *GFP* in E10.5 *Tshz1*$^{-/-}$ embryos reproduced that of endogenous *Tshz1*. The targeted allele contains only a short stretch of *Tshz1* coding sequence, devoid of putative functional domains of the protein, and should therefore behave as a null allele. The lack of *Tshz1* expression in null mutants was verified by in situ hybridization on whole mount embryos at mid embryogenesis (Fig. 1D) or on tissue sections at late stages (data not shown).

Tshz1 inactivation leads to neonatal lethality

Homozygous pups were obtained at a normal mendelian ratio at birth. However, none of the homozygous animals survived beyond P0 (Table 1). Careful examination of the *Tshz1*-deficient pups revealed that homozygous mutant mice exhibited a bloated abdomen and that no milk was present in

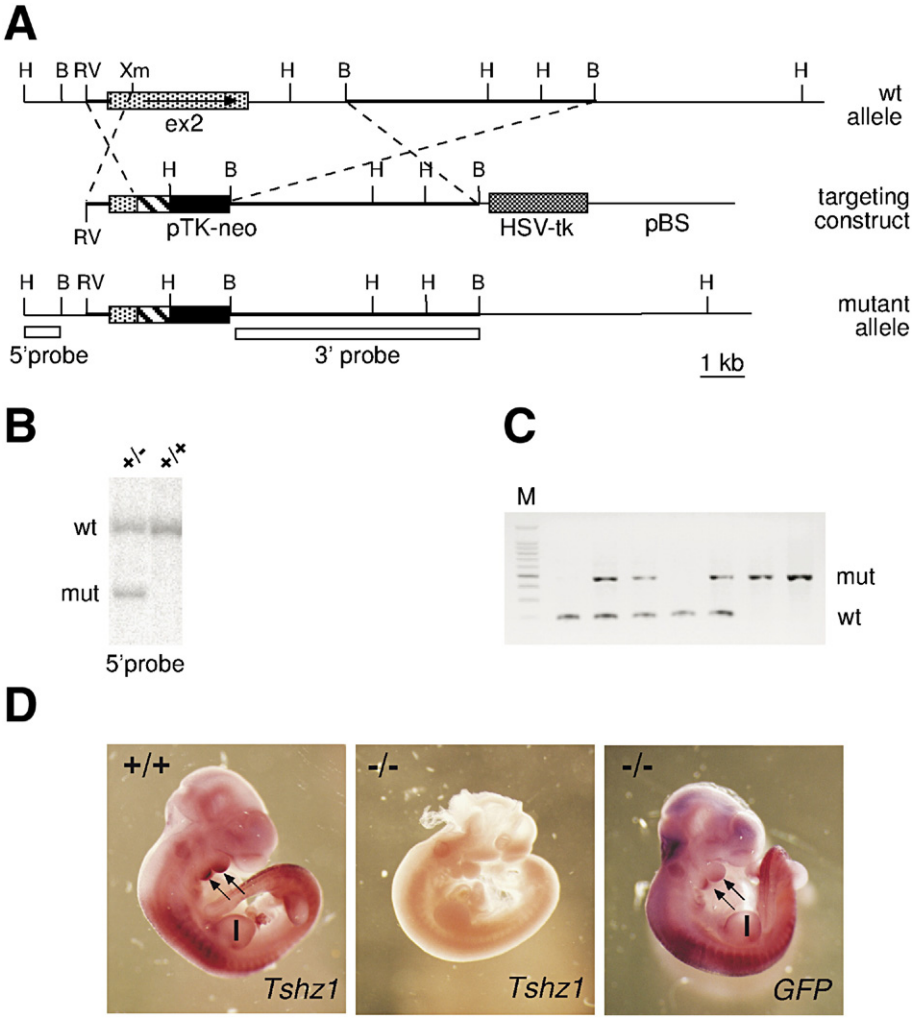

Fig. 1. Targeted disruption of *Tshz1*. (A) Schematic representation of a portion of the *Tshz1* locus from the wild type (top) and the targeted (bottom) alleles. The *Tshz1* open reading frame (ORF) is depicted as light dotted bars. Hatched bars represent the GFP ORF; black bars represent the neomycine resistance selection cassette (pTK-neo); dark dotted bars represent the herpes simplex virus thymidine kinase gene cassette (HSV-tk). The location of the 5′ external probe used for Southern blotting is indicated as a white bar. Restriction sites: B, *Bam*HI; H, *Hin*dIII; RV, *Eco*RV; Xm, *Xmn*I. (B) Genomic DNA from ES cells was digested by *Hin*dIII and hybridized using the 5′ external probe. The fragments generated from the wild type (wt) and the recombinant (mut) alleles are indicated on the left side of the panel. (C) PCR-based genotyping of animals from a F1 litter at P0. Lane 1 corresponds to the DNA size marker (M). Lanes 2 and 5 correspond to wild type animals, lanes 3, 4 and 6 correspond to heterozygotes and lanes 7 and 8 correspond to homozygotes. (D) In situ hybridization on wild type (+/+) and *Tshz1* homozygous (−/−) whole mount embryos at 10.5 dpc using *Tshz1* (left and middle) and *GFP* (right) as riboprobes. Note the absence of the *Tshz1* transcript in the *Tshz1*$^{-/-}$ embryo. The *GFP* expression pattern in *Tshz1*$^{-/-}$ embryo mimics that of *Tshz1* in wild type embryo with expression in the first and second branchial arches (arrows), in the neural tube and the somites and in the limb bud (l).

their stomachs (Fig. 2A). Dissection of the abdomen revealed that the gastro-intestinal apparatus was filled with air, from the esophagus to rectum, in addition to the peritoneal cavity (Figs. 2B, C). In addition, mutant pups suffered from respiratory distress. They frequently opened their mouth to seek air and we noticed high-speed contractions at the level of the diaphragm. Homozygous mutant newborns were unable to feed. Mutant analysis was initially performed on littermates of the F1–F2 generation established on C57BL/6J genetic background. It has been well documented that the genetic background can modulate the penetrance of mutant phenotypes (Barthold, 2004). Therefore, we tried to bypass the precocious lethality by crossing the *Tshz1* heterozygotes with CD-1 mice, a more robust outbred strain. Changing the genetic background did not influence lethality (Table 1) or other *Tshz1*-null associated phenotypes, even after six generations of breeding. We chose to pursue our mutant analysis with the CD-1 strain for which litters are more numerous than C57BL/6J line.

Table 1
Tshz1 mutants die at birth

Genetic background	No. of pups (total)	No. of dead pups at P0/total		
		Wild type	Heterozygous	Homozygous
		+/+	+/−	−/−
Mixed 129/Ola×B6	53	1/17	1/22	14/14
Mixed 129/Ola×CD-1 [a]	112	1/28	1/58	26/26

[a] Progenies obtained after 6 generations of backcross on CD-1 strain.

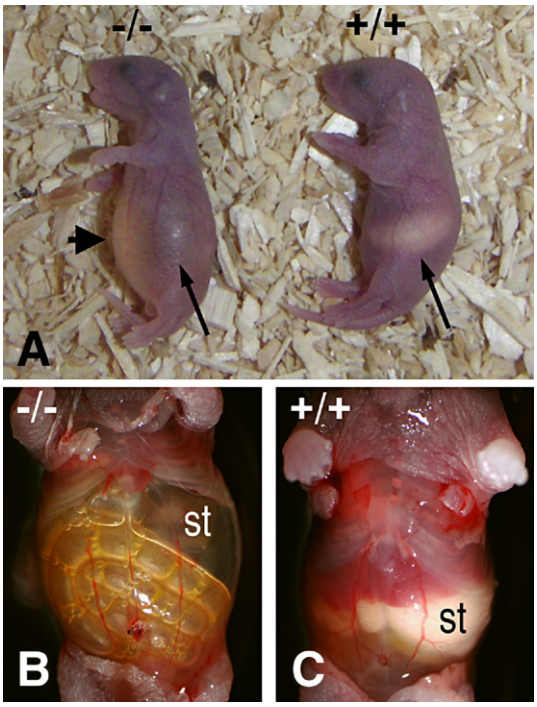

Fig. 2. Neonatal lethality of *Tshz1*-deficient mice. (A) *Tshz1*-deficient mice (−/−) die at birth and are characterized by a bloated abdomen (arrow head), compared to wild type newborns (+/+). Note the absence of milk in the stomach of (−/−) pup (arrow). (B, C) Enlarged focus of abdomens revealed that the intestine and the stomach (st) are completely filled of air in the (−/−) newborn compared to (+/+).

Palatal defects in Tshz1-deficient mice

In order to evaluate whether the inactivation of *Tshz1* function could alter organogenesis, we performed a gross morphological analysis of *Tshz1*$^{-/-}$ mutants from E17 to P0. The different organs were present and appeared normal and no tissues seemed to be disorganized. To understand the causes of the massive air entry through the esophagus in the *Tshz1*$^{-/-}$ newborns, we focused our analysis on the oral cavity. Interestingly, we detected a strong and fully penetrant defect in the region of the nasopharyngeal opening (Fig. 3). In wild type animals, the palate is composed of two parts: the hard palate in the anterior two/thirds and the soft palate in the posterior third. The hard palate corresponds to the bony component of the structure whereas the soft palate is composed of the palatal muscles and palatal aponeurosis, which is actually the extended tendon of the tensor veli palatini muscle. The soft palate separates the nasopharynx from the oropharynx and acts as a flap-valve to allow continuity between these two regions during breathing or to separate them during swallowing. Caudal to the soft palate, the epiglottis allows the passage of air through the larynx and prevents food and liquid entry into the trachea during swallowing. Histological staining of sections revealed shortening of the soft palate in the *Tshz1*$^{-/-}$ newborns (Figs. 3A, B), leading to a premature and enlarged entrance to the pharynx (Figs. 3O–T). Additionally, in the posterior region, the palatal structure of *Tshz1*$^{-/-}$ animals appeared thicker than control embryos and ended abnormally distant from the epiglottis with a bulbous shape. Moreover, the epiglottis appeared abnormal, presenting a flattened and stunted shape (Figs. 3P, Q, S, T). We inspected the morphology of the mouth and oral cavity of *Tshz1*$^{-/-}$ mutants at P0 (data not shown) and confirmed that the hard palate had fused properly giving rise to a normal pattern of rugae whereas the posterior part of the palate (velum) was missing. Examination of the Alizarin red and Alcian blue staining of P0 skulls showed that the palatine processes of the maxilla and the horizontal plates of the palatine bones, which compose the bony part of the palate, were not affected in the *Tshz1* mutant (data not shown). We examined the morphology of the oral cavity at earlier embryonic stages during formation of the secondary palate (Figs. 3C–N). We observed that the palatal shelves failed to fuse in their caudal most part in E14.5 *Tshz1*$^{-/-}$ embryos (Figs. 3G, H) whereas rostrally, fusion occurred normally (Fig. 3F). Later, after completion of fusion, the posterior extension of the palate was still lacking (Fig. 3N), demonstrating that the shortening of the soft palate did not result from developmental delay in the course of palate formation. We then looked at the expression of *Tshz1* in the developing palate from E12.5 to E14.5 and noticed that *Tshz1* was not detected in the palatal shelves (data not shown), suggesting that the contribution of this gene to the formation of the posterior palate takes place during early embryogenesis within the branchial arches.

Skeletal abnormalities in Tshz1-deficient mice

In *Drosophila*, *teashirt* (*tsh*) and *Hox* genes cooperate during embryogenesis to establish trunk segmental identities (de Zulueta et al., 1994; Roder et al., 1992). *Drosophila* embryos lacking *tsh* function are lethal and present homeotic transformation in the trunk epidermis. In vertebrates, *Hox* genes play an essential role in specification of the axial

Fig. 3. Development of the palate in wild type and *Tshz1*-deficient animals. (A, B) Histological analysis of sagittal head sections from wild type (−/−) and *Tshz1*$^{-/-}$ (−/−) newborns. The posterior palate (velum) is shorten in *Tshz1* homozygotes and leads to an enlarged entrance to the pharynx (B, arrow head), whereas in (+/+) the extremity of the posterior palate is closed to the epiglottis (A). Note the thick and bulbous shape of the posterior part of the mutant palate (B, arrow). (C to T) Series of frontal sections from ventral (left) to dorsal (right), focused on the palatal region of wild type (+/+) and mutant (−/−) embryos. Palate formation in 14.5 dpc wild type (C to E) and mutant (F to G) embryos. In (+/+), the palatal shelves (ps) have elevated to the horizontal position above the tongue (t) and have fused at the midline. In (−/−), fusion has normally occurred in the anterior part (F) but palatal shelves progressively failed to fused in the posterior part (G, arrow; H, asterisk). At 15.5 dpc (I to N), when the fusion is completed, the palate (p) separates the naso-pharynx (np) from the oropharynx (op) (I to K). Note the absence of the soft palate in *Tshz1*$^{-/-}$ embryos (L to N) resulting in abnormal communication between the naso- and oropharynx (N). The arrow in panel M reveals a partial fusion between the palatal shelves in a preceding section. (O to T) Sections from 17.5 dpc wild type (O to Q) and *Tshz1*$^{-/-}$ (R to T) embryos. The epiglottis (ep) appears flattened in the *Tshz1* mutant (arrow). Cartilages were revealed by Alcian blue staining. b, brain.

skeleton. *Tshz1* is expressed in the somites along the antero-posterior axis of the embryo with an anterior limit of expression coinciding with the occipital–cervical boundary (Caubit et al., 2000). Comparative analysis of *Tshz1* and *Pax-9* expression domains demonstrated that *Tshz1* was expressed in the sclerotome that gives rise to the future vertebrae (data

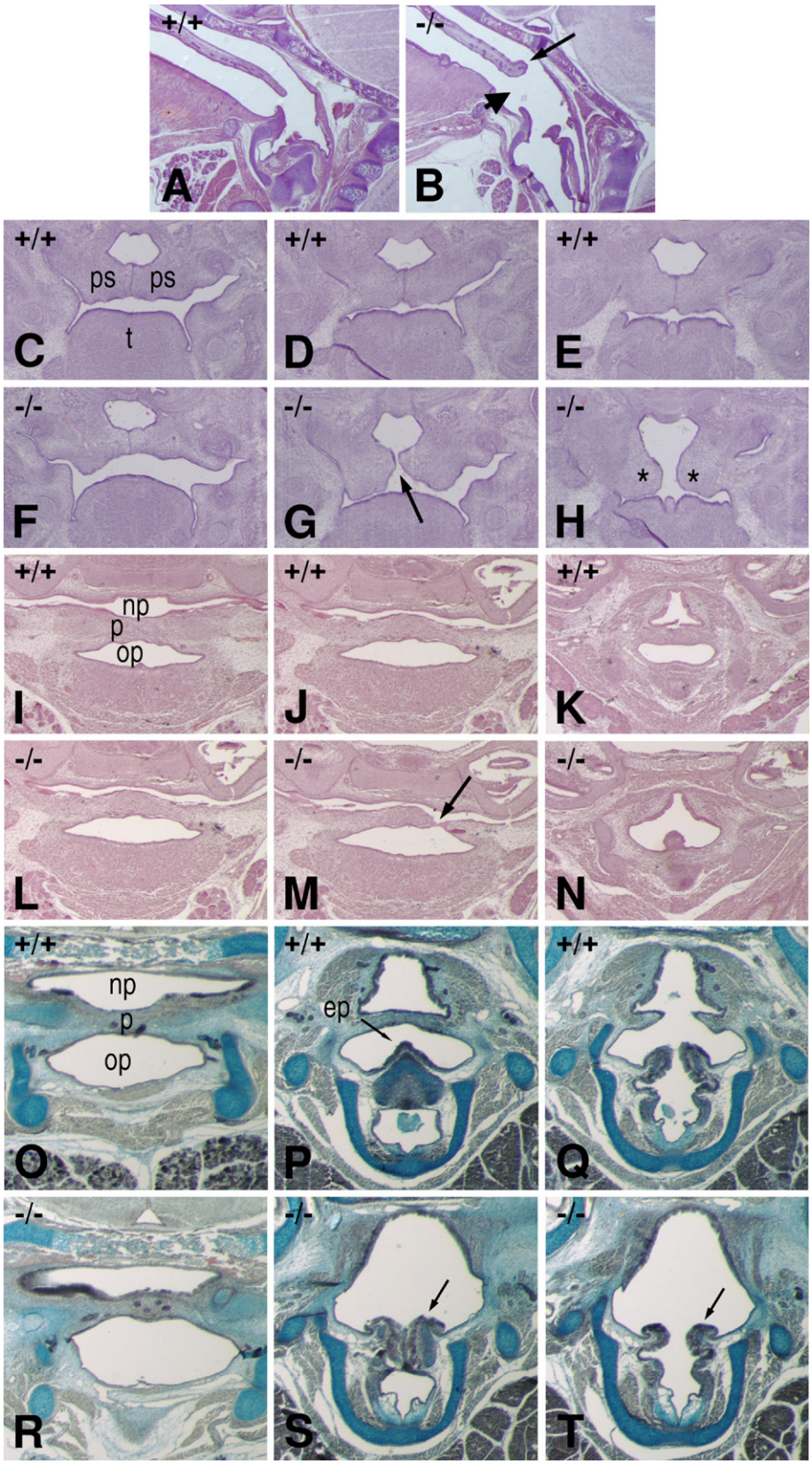

not shown). In order to evaluate the potential contribution of *Tshz1* in axial skeleton patterning, we examined skeletal preparations of control and mutant newborns (Fig. 4) (Table 2). We observed that *Tshz1*$^{-/-}$ mice displayed a number of different malformations of the cervical vertebrae, predominantly at the level of the axis (C2). The most penetrant

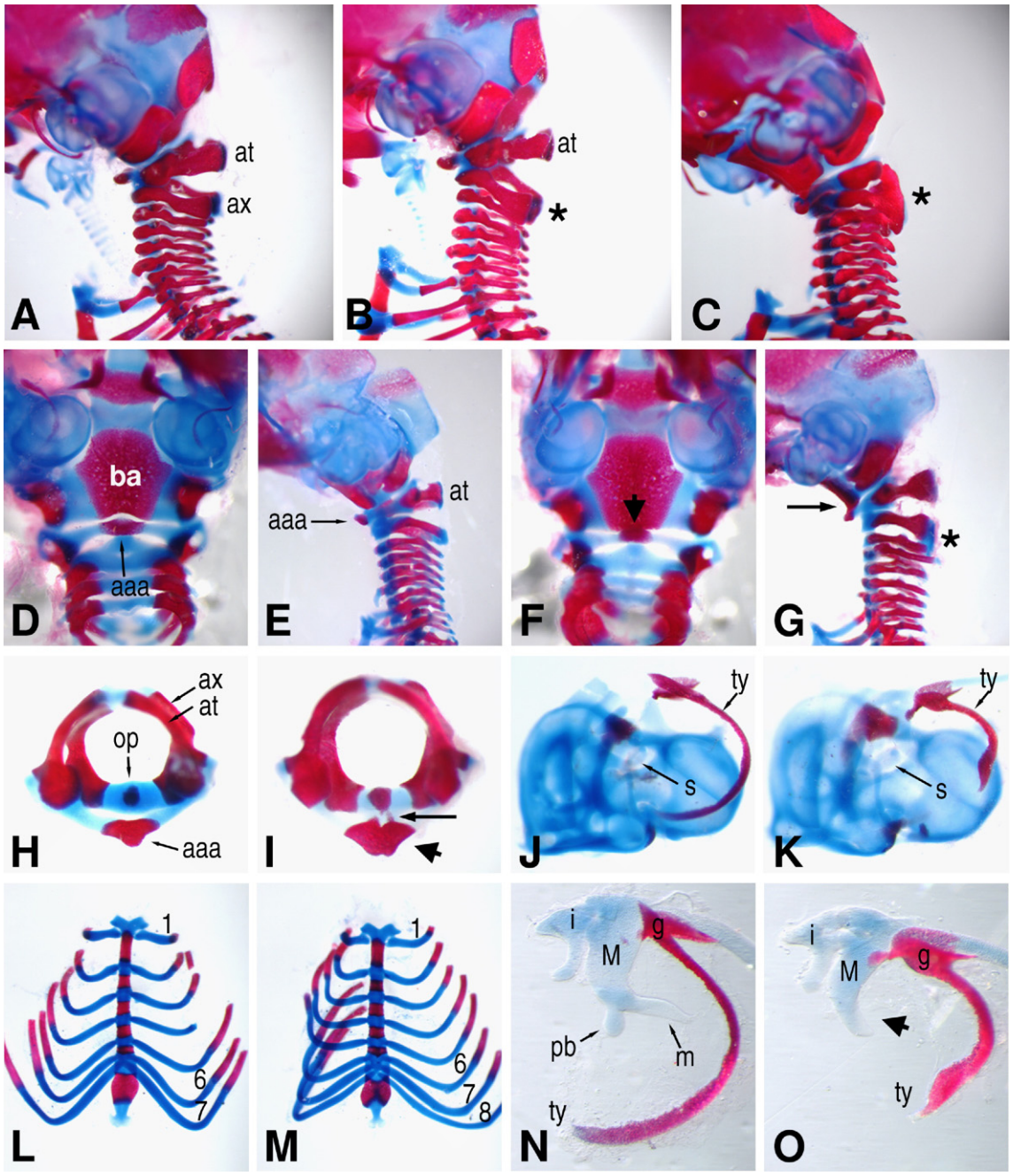

Fig. 4. Skeletal malformations in *Tshz1*-deficient mice. Bones and cartilages were revealed respectively by Alizarin red and Alcian blue staining. All panels correspond to animals at P0 except for (D to G) that correspond to 16.5 dpc fetuses. Lateral views of cervical vertebrae of wild type (A) and *Tshz1*$^{-/-}$ (B, C) skeletons. In wild type (+/+), 7 vertebrae are present in the cervical region with the first two vertebrae, the atlas (at) and the axis (ax) adopting a specific shape. In *Tshz1* mutant (−/−), vertebrae exhibit abnormal fusion of the neural arches (asterisks). The most frequent fusion occurs between the second (ax) and the third vertebrae as illustrated in panel B. In some cases, stronger defect resulting from dorsal fusions between the first 3 vertebrae is observed (C). (D–F) Ventral and (E–G) lateral views of cervical vertebrae. In (−/−), ectopic ossification leads to the abnormal fusion of the anterior arch of the atlas (aaa) to the basioccipital bone (ba) (F–G, arrow head and arrow), compared to (+/+) (D, E). (H, I) Superior views of atlas and axis. In (+/+), the two vertebrae are structurally independent (H) whereas in (−/−) the odontoid process (op) of the axis is now fused to the dorsal facet of anterior arch of the atlas (aaa) (I, arrow). In addition, the aaa is misshapen (arrow head). (L, M) Ventral views of the sternum. In (+/+), ribs from T1 to T7 are attached ventrally to the sternum (L), whereas ribs from T8 to T13 end freely. In (−/−), rib 8 is attached to the sternum at the same site of ribs 6 and 7 (M). Ribs 1, 6, 7 and 8 are indicated. Global views of the ear apparatus dissected from (+/+) (J) and (−/−) (K) mice. (N, O) Structural components of the middle ear. Dermal bones and cartilages are affected in (−/−) animals. The tympanic ring (ty) is shorter and thicker compared to (+/+) (N), the gonial bone (g) is altered and exhibits variable hypoplasia, the malleus body (M) is narrower and lacks the manubrium (m) and the processus brevis (pb) (O, arrow head). The incus (i) is normal as well as the stapes (s) which is properly positioned into the oval window (J, K).

Table 2
Summary of skeletal abnormalities in *Tshz1*$^{-/-}$ mutants

	Genotypes		
	+/+ (n=8)	+/− (n=8)	−/− (n=12)
Middle ear defects	0	0	12
Ventral fusion basioccipital-aaa‡	0	0	4
Ventral fusion C1–C2	0	1†	3
Abnormal neural arch at C2	0	1	11
Neural arches fusion at C2–C3	0	0	9+2*
8 vertebro-sternal ribs	1*	1*+1†	5

Values in columns correspond to number of animals. ‡Anterior arch of atlas. *Unilateral. †Same individual.

phenotype concerned the neural arch of C2, which is wider in the *Tshz1* mutants than in control mice. In addition, homozygotes exhibited a bilateral (75%) or unilateral (16%) fusion of the dorsal cartilage between the neural arches of C2 and C3 (Figs. 4A, B). Less frequently, fusions between C1 and C2 or C1, C2, and C3 were detected on both sides of the dorsal cartilage (Fig. 4C). Caudally, the morphology of the C4 to C7 cervical vertebrae appeared normal and thus seemed to be unaffected by the lack of the *Tshz1* function. In the ventral part of the cervical region, *Tshz1*$^{-/-}$ mutants presented abnormal fusions at a lower frequency. In 33% of *Tshz1*$^{-/-}$ mice, we noted an ectopic ossification that fused the caudal edge of the basioccipital bone to the anterior arch of the atlas (C1) (Figs. 4D–G). Interestingly, a similar fusion has been previously described in *Hoxd4* deficient mice (Horan et al., 1995). In wild type mice, C1 and C2 vertebrae are unconnected but the odontoid process of the axis (C2) projects anteriorly into the fovea dentis, a circular facet of the atlas, creating a rotary joint. In the absence of *Tshz1*, the atlas and the axis were often fused ventrally by an ectopic cartilaginous bridge with variable penetrance between the odontoid process and the anterior arch of the atlas (Figs. 4H, I). In addition, the anterior arch of the atlas was misshapen, appeared broader and was often split in the dorsal edge. In the thoracic region of wild type mice, ribs 6 and 7 were attached to the sternum at the same cartilaginous site between the 5th sternebra and the xyphoid process, and the 8th pair of ribs ends freely. In 5 out 12 *Tshz1*$^{-/-}$ mice, the 8th pair of ribs was abnormally attached to the sternum with the 6th and 7th ribs (Figs. 4L, M). In 2 out 5 of these animals, an ectopic ossification center developed, giving rise to an additional sternebra between ribs 7 and 8 (data not shown). These results reveal the anterior transformation of the T8 vertebra, which acquires T7 identity in the absence of *Tshz1*. A similar homeotic phenotype has been observed in *Hoxc8* and *Hoxc4* deficient mice (Boulet and Capecchi, 1996; Le Mouellic et al., 1992). More caudally, *Tshz1* function seems to be dispensable to skeletal morphogenesis since we did not detect any malformation in lumbar and sacral vertebrae. In addition, although *Tshz1* is expressed in the limb bud mesenchyme, the ossified and cartilaginous structures of the limbs developed correctly in *Tshz1* mutants (data not shown).

To determine whether the vertebral defects observed in *Tshz1*$^{-/-}$ mutants could result from a deregulation of *Hox* gene expression, we analyzed the expression pattern of *Hoxd4* and *Hoxc8* in *Tshz1*$^{-/-}$ embryos. No alteration in the anterior–posterior limit and in the level of *Hoxd4* and *Hoxc8* expression was detected in the somitic mesoderm in the absence of *Tshz1* (Fig. 5), indicating that *Tshz1* does not control the maintenance of Hox genes expression in the somites.

Tshz1 is required for formation of the middle ear

We have previously described the expression pattern of *Tshz1* in the branchial arches during embryogenesis (Caubit et al., 2000). *Tshz1* is expressed from E9.5 in the neural crest-derived mesenchyme in the posterior part of the mandibular arch and the anterior part of the second arch (BA2). In addition, *Tshz1* is expressed within a thin layer in the proximal portion of the epithelium lying between the maxillary and mandibular components of the 1st branchial arch (BA1). In this study, we examined in more detail the expression pattern of *Tshz1* by in situ hybridization on tissue sections at different embryonic stages in the branchial arches and derived structures.

The craniofacial skeleton largely derives from the neural crest cells that migrate and differentiate into the branchial arches (Santagati and Rijli, 2003). We examined bones and cartilages in the skull of *Tshz1*$^{-/-}$ newborns to detect potential craniofacial defects. Strikingly, we found fully penetrant malformations in the craniofacial skeleton, specifically in middle ear components. We did not detect any malformation of the other ossified or cartilaginous structures. The middle ear apparatus is composed of three ossicles that are generated by endochondral ossification, the malleus, incus and stapes and of

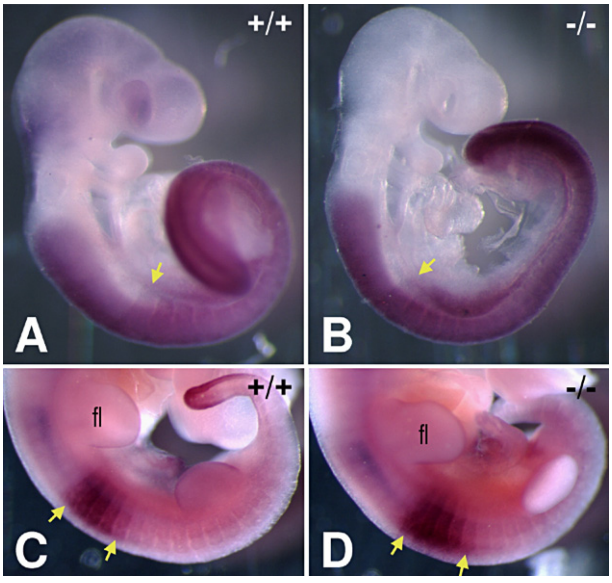

Fig. 5. Expression of *Hox* genes in *Tshz1*-deficient embryos. In situ hybridization on whole mount embryos at 10.5 dpc using (A, B) *Hoxd4* and (C, D) *Hoxc8* riboprobes. The anterior limits of expression of both *Hoxd4* and *Hoxc8* are set at the same somitic boundary in (A, C) wild type (+/+) and (B, D) *Tshz1*-null (−/−) embryos as indicated by arrows. Six to seven embryos of each genotype were used for each probe. fl, forelimb.

two membranous bones, the tympanic ring and the gonium (Mallo, 2003). The malleus is composed of a main body with different processes attached to it, including the manubrium and the processus brevis. The manubrium is a key component of the middle ear apparatus as it connects the ossicle chain with the tympanic cavity through its insertion into the tympanic membrane. In the *Tshz1*$^{-/-}$ mice, the malleus presented an abnormal shape accompanied by the lack of the manubrium and processus brevis (Figs. 4N, O). The proximal part of the malleus developed normally except that the main body was significantly narrower. The distal part was completely disrupted and ended prematurely with a claw-like tip. In addition, the tympanic ring was strongly shortened, thicker than normal and ended with a blistered shape. The gonial bone presented variable hypoplasia and abnormal shape. By contrast, the incus and the stapes developed normally as did the joints between the 3 ossicles, and the stapes was correctly inserted into the oval window (Figs. 4J, K). Histological analysis of the ear region (Fig. 6) confirmed the shortening and the abnormal position of the tympanic ring, which was displaced laterally. In the manubrial area, the *Tshz1*$^{-/-}$ ear exhibited a small rounded cartilaginous structure between the external acoustic meatus (EAM) and the tubo-tympanic recess (Figs. 6A, C). The formation of the EAM was induced appropriately in the *Tshz1*$^{-/-}$ mutant but was shorter as a likely consequence of the lateral displacement of the tympanic ring (Figs. 6B, D).

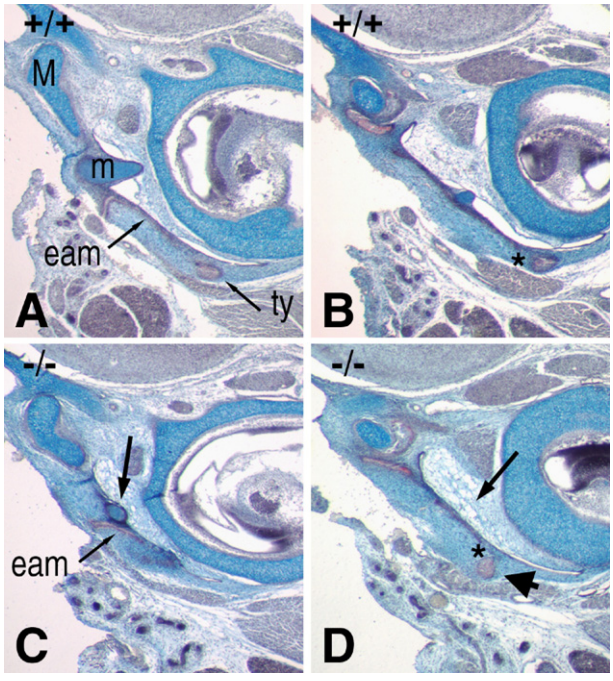

Fig. 6. Histological analysis of the middle ear of wild type and *Tshz1*-deficient fetuses. Frontal sections from ventral (A–C) to dorsal (B–D) at 17.5 dpc. Membranous (red) and endochondral (blue) bones are distinguished respectively by Sirius red and Alcian blue staining. (A, B) In wild type (+/+), the manubrium (m) of the malleus (M) is inserted between the external acoustic meatus (eam) and the middle ear cavity. (C, D) In Tshz1-null fetuses (−/−), the manubrium is absent (arrow) in dorsal view. Note, in ventral view (C), the presence of a small cartilaginous structure (arrow) which corresponds to the craw-like tip of the malleus, as illustrated in Fig. 4O. The tympanic ring (ty) is absent in ventral view and displaced laterally in dorsal view (arrow head). The extremity of the eam is correlated to the position of the tympanic ring (B–D, asterisks). Lateral is to the left, anterior to the top.

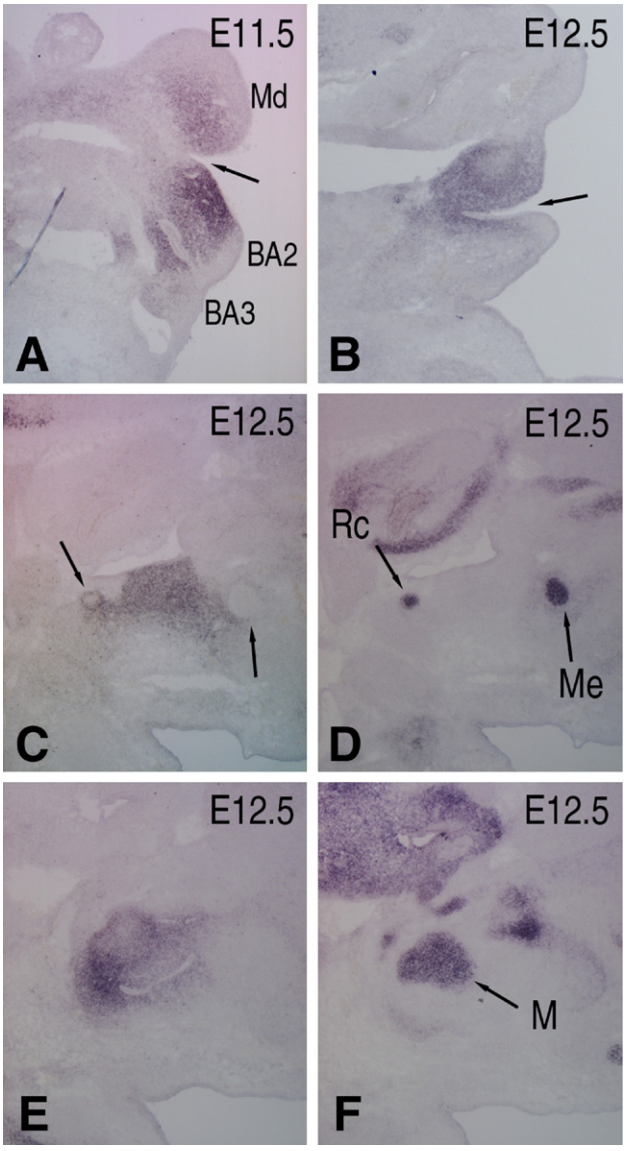

Fig. 7. Expression of *Tshz1* and *Sox9* during early middle ear development. (A) *Tshz1* expression in the mesenchyme of the branchial arches at 11.5 dpc. Transverse section, dorsal to the top. The arrow indicates the first pharyngeal cleft. Md, mandibular; BA2, second and BA3, third arches. (B) *Tshz1* expression in frontal section at 12.5 dpc, anterior to the top. The arrow indicates the meatal plug. *Tshz1* is expressed on both sides of the meatus and around the malleal primordium. (C–F) Comparative analysis of *Tshz1* (C, E) and *Sox9* (D, F) expression at 12.5 dpc. Adjacent sagittal sections. Anterior to the top, dorsal to the left. *Sox9* is expressed in the malleal primordium (M) and in the developing Meckel's (Me) and Reichert's (Rc) cartilages. *Tshz1* is expressed complementary to *Sox9* in the mesenchyme surrounding the developing malleus (E), the Me and Rc cartilages (C, arrows) and in the mesenchyme adjacent to the meatus, on both sides.

The middle ear defects induced by the lack of *Tshz1* function in embryos were closely correlated with the expression pattern of *Tshz1* in the branchial arches (Fig. 7A). To assess whether middle ear defects could be result of a mis-specification of mesenchymal progenitors in branchial

arches, we examined branchial arch development in *Tshz1*$^{-/-}$ embryos between E9.5 and E11.5. The morphology of the branchial arches appeared normal as illustrated in Fig. 1, and, furthermore, we were unable to detect any change in the expression pattern of a number of genes involved in the specification of these structures (Supplementary Fig. 1). Together, these results indicate that *Tshz1* is not required to control the early patterning of the first and second branchial arches but rather specifically controls the development of the middle ear.

From E12.5, *Tshz1* was expressed in the mesenchyme of the developing middle ear, within areas surrounding the condensing malleus and tympanic ring and on both sides of the EAM (Figs. 7B, C, E). Comparative analysis using *Sox9*, an early marker of cartilage differentiation, demonstrated that *Tshz1* was excluded from the cartilaginous condensation but rather bordered and surrounded the future cartilages (Figs. 7C–F). The overt differentiation of the malleus occurs between E12 and E14.5 (Mallo et al., 2000). We then examined the expression pattern of *Sox9* in the *Tshz1*$^{-/-}$ developing middle ear at these different stages. At E14.5 (Figs. 8A–D), *Sox9* mRNA was detected at normal level in the chondrogenic zones of the middle ear. However, we observed that the spatial domain of *Sox9* expression was clearly altered in the differentiated malleus in *Tshz1* mutant embryos. While in wild type embryos, the manubrium was distinguishable from the main body of the malleus and extended medially to contact the tympanic membrane (Figs. 8A, C), in *Tshz1* mutant embryos the malleal structure developed as a compact masse without identifiable manubrium and processes (Figs. 8B, D). As soon as E12.5, the expression domain of Sox9 was strongly reduced in size, leading to a smaller malleal primordium in the absence of *Tshz1*. These results demonstrate that *Tshz1* does not control the transcriptional level of *Sox9* and then the differentiation of chondrogenic precursors but rather seems implicated earlier in the formation of the condensing malleal primordium.

Since other mutants exhibit malformations of the middle ear apparatus, we examined, in *Tshz1*$^{-/-}$ embryos, the expression of genes known to play a role in the formation of the malleus, the EAM and the tympanic ring. In *Goosecoid (Gsc)*-deficient mice, the EAM fails to develop, the tympanic ring is absent and the malleus is greatly affected and lacks the manubrium (Rivera-Perez et al., 1995; Yamada et al., 1995). Mice lacking *Msx1* function present malformations of the malleus mainly characterized by the absence of the processus brevis (Zhang et al., 2003). Milder anomalies were detected in *Bapx1*-null mutants where the width of the malleus was slightly reduced and the gonium and anterior tympanic ring were hypoplastic (Tucker et al., 2004). In the absence of *Tshz1*, *Msx1* and *Gsc* were still expressed in the mesenchyme surrounding the developing malleus (Figs. 9A–D). Likewise, the expression of *Bapx1* around the Meckel's cartilage and surrounding the malleus was unaffected in *Tshz1*$^{-/-}$ embryos (Figs. 9E–H). We concluded that the middle ear defects generated in the absence of *Tshz1* were not due to the deregulation of *Msx1*, *Gsc* or *Bapx1* during the formation of this structure.

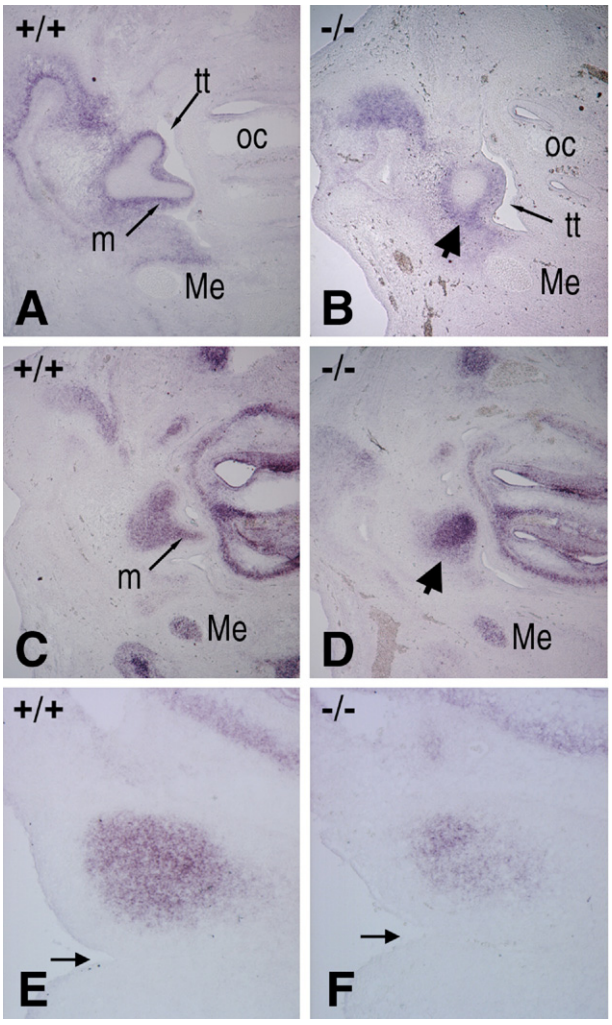

Fig. 8. Expression of *Sox9* in the developing malleus of *Tshz1*-deficient embryos. (A, C) Wild type (+/+) and (B, D) *Tshz1* homozygous (−/−) embryos at 14.5 dpc. Transverse sections; dorsal to the top, lateral to the left. In (+/+), the expression of *Tshz1* around the chondrogenic area (A) of the developing malleus is complementary to that of *Sox9* (C). (B) Expression of *GFP* and (D) *Sox9* reveals the structural alteration of the manubrial chondrogenic area (arrow head) in (−/−) embryos. m, manubrium; Me, Meckel's cartilage; oc, otic capsule; tt, tubo-tympanic recess. (E, F) Earlier, at E12.5, the expression domain of Sox9 in the malleal condensation area presents a size reduction in Tshz1-null mutant embryos (F) compare to wild type (E). Frontal sections, rostral to the top, lateral to the left. The arrow indicates the first branchial cleft.

Since the gonium and the tympanic ring arise from dermal ossification, we examine the expression of *Cbfa1/Runx2* as a marker of developing bones, in *Tshz1*-null embryos. In mice, expression of *Cbfa1* has been described by E12.5 in mesenchymal tissue around the condensation of the Meckel's cartilage (Ducy et al., 1997), but no expression in the primordia for the gonium and the tympanic bone was depicted. However, it has been described that the primordium for the tympanic ring forms by E13.5 as a condensation ventral to the first pharyngeal cleft, lateral to the Meckel's cartilage (Mallo and Gridley, 1996). The analysis of the expression pattern of *Cbfa1* between E12.5 and E13.5 in *Tshz1*$^{-/-}$ embryos (Figs. 9I–L) showed that although the expression surrounding the Meckel's condensation is unaffected, we observed the

alteration of a *Cbfa1* expressing area lying caudal to the tubo-tympanic recess and lateral to the Meckel's cartilage, within a mesenchymal region where *Tshz1* is normally expressed (Fig. 7C). At E12.5, *Cbfa1* is undetectable in this area in the absence of *Tshz1* and is weakly detected later on at E13.5, suggesting that expression of *Cbfa1* could be downregulated or simply delayed in the *Tshz1*-null mutant. This *Cbfa1* expressing domain was adjacent to *Bapx1* expressing domains that have been described to correspond to the condensing tympanic bone and gonium (Tucker et al., 2004). This result suggests that the malformation of the tympanic ring and gonium in the *Tshz1* mutant could result from a mis-regulation of *Cbfa1*.

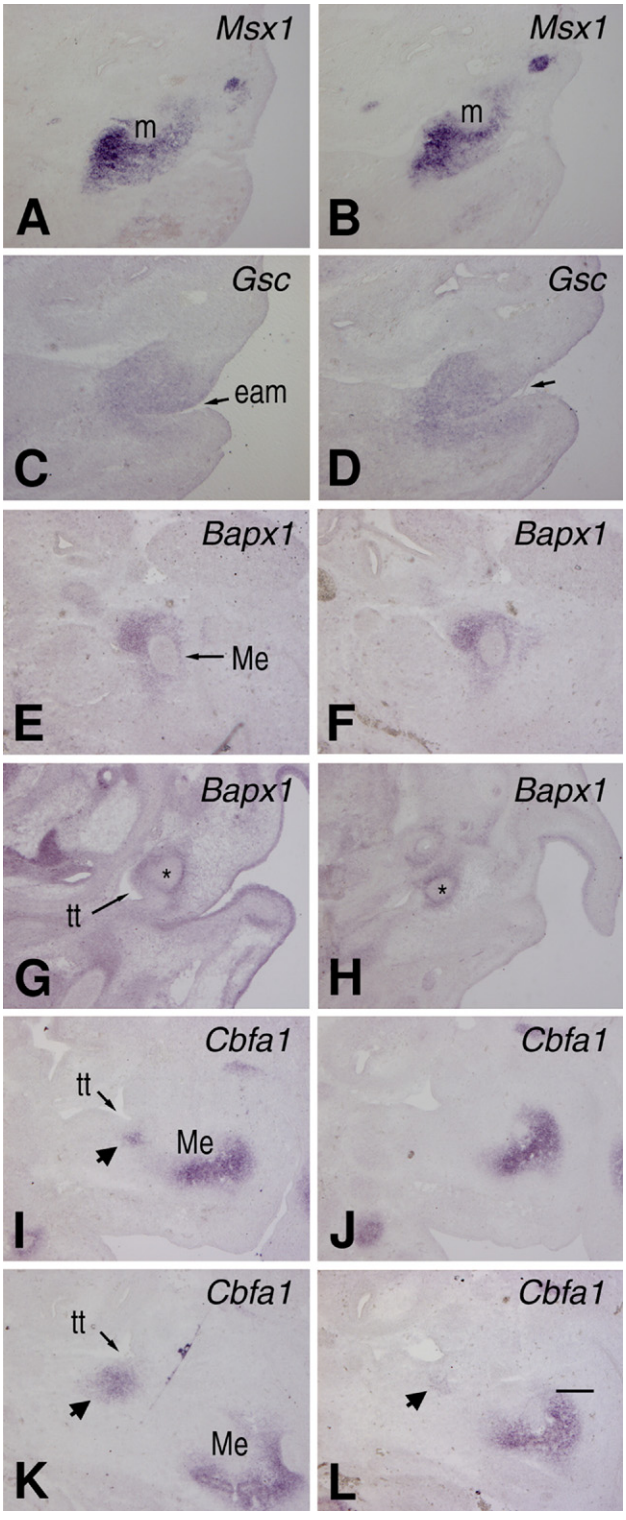

Discussion

In this study, we described the first functional analysis in mouse of a member of the *Tshz* gene family. We demonstrated that the invalidation of *Tshz1* induces neonatal lethality, accompanied by a range of developmental defects. First, *Tshz1*$^{-/-}$ newborns exhibit a specific defect of the soft palate. Second, *Tshz1*$^{-/-}$ axial skeletons present malformations of several vertebrae in the cervical and thoracic regions reminiscent of Hox mutant phenotypes. Finally, the *Tshz1*-null mutation induces restricted malformations of structural components of the middle ear apparatus. Together, these results demonstrate that *Tshz1* plays an essential role in multiple processes during mouse development.

Tshz1 is required for the formation of the soft palate

Shortly after birth, *Tshz1*$^{-/-}$ animals exhibit a distended abdomen resulting from massive air entry through the digestive tract. It has been reported that targeted deletion of a number of developmental genes presented a phenotype of neonatal lethality accompanied by an air-filled digestive tract that in some cases leads to a distension of the abdomen. For the majority of these mutants, the accumulation of air in the stomach and intestine was correlated with a cleft of the secondary palate (Bi et al., 2001; Peters et al., 1998; Qiu et al., 1997; Satokata and Maas, 1994; Shamblott et al., 2002; ten Berge et al., 1998; Winograd et al., 1997). However, in other mutants, the phenotype of bloated abdomen was associated with other developmental defects such as ankyloglosia (Morita et al., 2004) or respiratory failure due to lung and tracheal defects (Aubin et al., 1997). Finally, a bloated abdomen was associated with an anomaly of the soft palate in *Hoxa3* mutant mice (Chisaka and Capecchi, 1991). In *Hoxa3* deficient mice, the soft palate is truncated and thus is unable to function as a flap to separate the nasopharynx to the oropharynx. Moreover, the epiglottis cartilage is structurally altered and the muscles surrounding the throat appear disorganized. These defects, combined with

Fig. 9. Analysis of gene expression in the developing ear of *Tshz1*-deficient embryos. In situ hybridization on wild type (A, C, E, G, I, K) and *Tshz1*$^{-/-}$ (B, D, F, H, J, J) embryos. The mesenchymal expression of *Msx1* (A, B) and *Gsc* (C, D) surrounding the developing malleus (m) is unaffected in the absence of *Tshz1*. Frontal sections E13.5. In situ for *Bapx1* on sagittal sections at E13.5 (E, F) and transverse sections at E14.5 (G, H) showing normal expression around the Meckel's cartilage (Me) and the manubrium of the malleus (asterisk). (I–L) Expression of *Cbfa1* on sagittal sections. Normal expression was detected around the Meckel's cartilage at E12.5 (I, J) and E13.5 (K, L). However, expression of *Cbfa1* in a group of mesenchymal cells (large arrowhead) caudal to the tubo-tympanic recess (tt) is undetectable at E12.5 (J) and strongly reduced at E13.5 (L) in the absence of *Tshz1*. eam, external acoustic meatus.

breathing failure, probably lead to a dysfunction of the air passages into the throat in *Hoxa3* mutants. On the other hand, *Sall3*, a member of the *Spalt* gene family, encoding a zinc finger protein, has also been reported to affect the posterior palate when inactivated in mice. However, in spite of these malformations, no phenotype of aerophagia was described (Parrish et al., 2004). Here we show that the inactivation of Tshz1 leads to premature truncation of the soft palate during palate formation. Strikingly, the palatal defect observed in the Tshz1-null mutant resembles that of *Hoxa3* and *Sall3* mutants. It is interesting to note that, in *Drosophila*, *Hox* and *spalt* genes genetically interact with *teashirt* (Roder, 1992; Roder et al., 1992). This raises the possibility that, in mouse, *Tshz1* may be implicated with *Hoxa3* and/or *Sall3* in a common pathway to control proper development of the posterior palate. In a first attempt to investigate this point, we examined the expression of *Sall3* and *Hoxa3* in *Tshz1*-null embryos (Supplementary Fig. 2). *Sall3* and *Hoxa3* were properly expressed in the posterior palate and the floor of the pharynx respectively (Gaunt, 1988; Parrish et al., 2004).

Very few genes have been reported to affect the posterior palate (velum) when mutated in mice and little is known about the early development of this structure. The soft palate has a layer of fibrous tissue, the palatine aponeurosis, which is attached to the posterior edge of the hard palate. All muscles of the soft palate are attached to this aponeurosis, which corresponds actually to the expanded tendon of the tensor veli palatini muscle. These muscles originate from cranial mesoderm or occipital somites that migrate into the branchial arches. *Tshz1* is not expressed in the developing palate from E12.5 onward. However, earlier in embryogenesis, *Tshz1* is expressed in branchial arch mesenchyme. It is thus likely that the palatal defect of *Tshz1* mutant mice is a consequence of the absence of *Tshz1* within the branchial arches. During the expansion of the branchial neural crest populations, interfaces are established with underlying mesoderm: the myogenic mesodermal core tissue is surrounded by the neural crest cells (NCC) and interactions between these two populations are required for organizing the myogenic as well as the skeletal and endothelial derivatives (Noden and Francis-West, 2006; Trainor and Tam, 1995; Tzahor et al., 2003). In this context, we propose that *Tshz1* may play a role in controlling interactions between the ectomesenchyme and the underlying mesoderm to trigger the differentiation of particular branchial myogenic structures such as the future muscles of the palate.

Tshz1 is required for axial skeletal morphogenesis

The vertebral column and the ribs develop from the sclerotomal compartment of differentiated somites. We show here that *Tshz1* inactivation leads to vertebral malformations in the axial skeleton, in agreement with its expression in the sclerotome during embryogenesis. This result demonstrates that *Tshz1* function is necessary for normal patterning of the axial skeleton. However, although *Tshz1* is expressed throughout the trunk somites, alterations of the *Tshz1*$^{-/-}$ skeleton are restricted to the cervical and thoracic vertebrae while the lumbar and sacral vertebrae developed correctly. The *Tshz1* mutation predominantly affects vertebrae at the morphological transition between occipital and cervical regions, which is consistent with the position of the anterior border of *Tshz1* expression domain within the somitic mesoderm (Caubit et al., 2000). We have previously shown that *Tshz2* transcripts are also detected in the developing somites in a more caudal domain. Consequently, the absence of malformations in the posterior region of the vertebral column could be due to overlapping functions of *Tshz2* and *Tshz1*. Inactivation of *Tshz2* will be a useful tool to substantiate this point in the future.

It is noteworthy that the morphological changes of vertebrae in *Tshz1* mutants are reminiscent of vertebral malformations induced by loss-of-function mutations that alter *Hox* genes expression, such as *Hoxd4* (Horan et al., 1995), *Hoxc4* (Boulet and Capecchi, 1996) and *Hoxc8* (Le Mouellic et al., 1992). In *Drosophila*, Teashirt protein is involved in the Hox network to control the development of various tissues. In the trunk region, it has been shown that Tsh is a downstream target of the trunk-specific Hox proteins (Mathies et al., 1994; McCormick et al., 1995), but also that Tsh behaves as a cofactor of Hox proteins to promote trunk versus head identity (de Zulueta et al., 1994; Roder et al., 1992). It could be thus possible that in mice, *Tshz1* and *Hox* genes are involved in common pathway to control the morphogenesis of the axial skeleton. Therefore, we propose that Tshz1 and some Hox proteins may interact to control common target genes to specify vertebral identity. Supporting this hypothesis, preliminary results from GST-pull down assays suggest that Tshz and some Hox proteins physically interact (I. Manfroid, unpublished data). In addition, in a nonexclusive hypothesis, *Tshz1* may be a downstream target of Hox proteins during the differentiation of somitic mesoderm.

Tshz1 is important for middle ear development

In mammals, the auditory system is composed of three distinct parts of different embryological origins. The outer and middle ears develop from the first and second branchial arches (Mallo, 2003) whereas the inner ear, which is the sensory component of the system, derives from the otic placode (Mallo, 2003; Morsli et al., 1998). Our present results clearly demonstrate that *Tshz1* is necessary for middle ear development and plays a role in the formation of key structures that allow the organization of a functional tympanic membrane. A hypothetical model has emerged from the literature, suggesting that the assembling of a functional tympanic membrane requires the coordinate development of different structures (Mallo and Gridley, 1996; Mallo et al., 2000). First, the tympanic ring is suspected to coordinate the invagination of the first pharyngeal cleft to form the EAM. The anatomical position of the EAM is consequently linked to that of the tympanic ring. Secondly, the EAM may provide signaling activities that are necessary to induce the development of the manubrium of the malleus by controlling chondrogenic differentiation of the underlying

mesenchyme. In particular, signals from the EAM are able to induce *Sox9* expression in the mesenchyme of the developing manubrial area although at a distance from the epithelium. Molecular links are therefore required to transmit the signals from the epithelium to the distant mesenchyme. It is remarkable that loss of *Tshz1* function affects both the development of the tympanic ring and the malleal manubrium. This result suggests that *Tshz1* may play a role in the different steps coordinating development of the middle ear apparatus. *Tshz1* is expressed in the mesenchyme adjacent to the epithelium of the EAM and in mesenchymal tissue surrounding the malleus and manubrium primordia, but is downregulated in the chondrogenic areas. Explant culture experiments have shown that *Tshz1* expression in the first branchial arch is under the control of epithelial factors, including Fgf8 and Bmp4 (Long et al., 2001). These data suggest that *Tshz1* is implicated in some aspect of the reciprocal interactions between the branchial arch-derived mesenchyme and the overlying epithelium that control induction of the tympanic ring and the manubrium. We show that inactivation of *Tshz1* leads to the deregulation of *Cbfa1* in mesenchymal condensation that presumably gives rise to the tympanic ring. This result suggests that the malleal defects induced in the *Tshz1*-null mutant could be the consequence of the primary malformation of the tympanic ring. However, the primordium of the tympanic ring is first apparent at E13.5 (Mallo and Gridley, 1996) and we showed that the malleal condensation is affected as soon as E12.5 in the absence of *Tshz1*. Therefore, we cannot exclude that in addition *Tshz1* could play a direct role in the formation of the malleus.

The development of the skeletal structures involves sequential phases; migration of the pre-skeletal mesenchymal cells to the final site of skeletogenesis; then condensation of these cells, resulting from interactions with the surrounding epithelial cells, that finally leads to differentiation of chondroblasts or osteoblasts (Hall and Miyake, 2000). We propose that *Tshz1* could play a role at the condensation stage, which is a crucial stage in skeletogenesis, by establishing the boundary and/or the size of the condensation. Indeed, *Tshz1* is expressed in mesenchyme surrounding condensations, a critical position to modulate expansion of condensation size.

Usually, regulatory genes expressed in the branchial arches during embryogenesis lead to several malformations within craniofacial cartilaginous and ossified structures when mutated. Here we show that inactivation of *Tshz1* leads to specific alteration of the middle ear apparatus. This result suggests that *Tshz1* function is not required for early patterning of the branchial arches but rather is specifically required to control the development of middle ear components. *Tshz1* thus probably acts downstream of the regulatory genes known to be implicated in the patterning and the differentiation of branchial arches-derived structures or acts as specific cofactor of regulatory molecules to ensure middle ear formation.

Congenital aural atresia (CAA) is a rare developmental anomaly of the ear, characterized by a conductive hearing loss with variable degree (Cremers et al., 1988; Strathdee et al., 1995). The ear abnormalities linked to CAA involve developmental failure of the external auditory canal, malformation of the tympanic membrane, the ossicles and the middle ear cavity. However, the inner ear of the patients appears to develop normally. Thus, CAA results from the abnormal development of the first and second branchial arches and the first branchial cleft. CAA has been frequently reported in patients with chromosomal anomalies on the long arm of chromosome 18 (18q) (Cody et al., 1999; Keppler-Noreuil et al., 1998; Kline et al., 1993). Recently, CAA syndrome was linked to a 2.3-Mb deletion on chromosome 18q22.3–18q23 (Dostal et al., 2006), delineated by the polymorphic markers D18S489 and D18S554. Although 9 genes have been mapped in this genomic region, none of them have been implicated in the cause of this syndrome. We found that the human *TSHZ1* (SDCCAG33) gene maps in this critical interval, 0.4 Mb distal to D18S489. We show here that inactivation of *Tshz1* in mouse leads to a severe middle ear phenotype, mimicking defects observed in the CAA syndrome in human. Therefore, we propose *TSHZ1* as one good candidate gene for CAA syndrome.

Acknowledgments

We thank V. Girod-David for excellent technical help. We are grateful to H. Cremer and R. Kelly for comments on the manuscript. We acknowledge the following colleagues for the generous gifts of probes: F. Watrin (*GFP*), K. Rizzoti (*Sox9*), F. Rijli (*Hoxa2, Gsc*), B. Robert (*Msx1*), V. Pachnis (*Lhx6*), P. Monaghan (*Sall3*), V. Lefèbvre (*Cbfa1*), T. Lufkin (*Bapx1*), M. Morasso (*Dlx3*), M. Seiweke (*Hoxa3*). We thank Lois J. Maltais and the Mouse Genome Nomenclature Committee (MGNC) and the HUGO Gene Nomenclature Committee (HGNC) that have approved the nomenclature for the *teashirt* gene family. This work was supported by grants from the Association Française contre les Myopathies (AFM), the Association pour la Recherche contre le Cancer (ARC) and by institutional funds from CNRS and INSERM. X.C. is member of the Université Aix-Marseille I.

Appendix A. Supplementary data

Supplementary data associated with this article can be found, in the online version, at doi:10.1016/j.ydbio.2007.05.038.

References

Alexandre, E., Graba, Y., Fasano, L., Gallet, A., Perrin, L., De Zulueta, P., Pradel, J., Kerridge, S., Jacq, B., 1996. The *Drosophila* teashirt homeotic protein is a DNA-binding protein and modulo, a HOM-C regulated modifier of variegation, is a likely candidate for being a direct target gene. Mech. Dev. 59, 191–204.

Aubin, J., Lemieux, M., Tremblay, M., Berard, J., Jeannotte, L., 1997. Early postnatal lethality in Hoxa-5 mutant mice is attributable to respiratory tract defects. Dev. Biol. 192, 432–445.

Barthold, S.W., 2004. Genetically altered mice: phenotypes, no phenotypes, and Faux phenotypes. Genetica 122, 75–88.

Bel, S., Core, N., Djabali, M., Kieboom, K., Van der Lugt, N., Alkema, M.J., Van Lohuizen, M., 1998. Genetic interactions and dosage effects of Polycomb group genes in mice. Development 125, 3543–3551.

Bel-Vialar, S., Core, N., Terranova, R., Goudot, V., Boned, A., Djabali, M.,

2000. Altered retinoic acid sensitivity and temporal expression of Hox genes in polycomb-M33-deficient mice. Dev. Biol. 224, 238–249.
Bessa, J., Gebelein, B., Pichaud, F., Casares, F., Mann, R.S., 2002. Combinatorial control of *Drosophila* eye development by eyeless, homothorax, and teashirt. Genes Dev. 16, 2415–2427.
Bi, W., Huang, W., Whitworth, D.J., Deng, J.M., Zhang, Z., Behringer, R.R., de Crombrugghe, B., 2001. Haploinsufficiency of Sox9 results in defective cartilage primordia and premature skeletal mineralization. Proc. Natl. Acad. Sci. U. S. A. 98, 6698–6703.
Boulet, A.M., Capecchi, M.R., 1996. Targeted disruption of hoxc-4 causes esophageal defects and vertebral transformations. Dev. Biol. 177, 232–249.
Caubit, X., Core, N., Boned, A., Kerridge, S., Djabali, M., Fasano, L., 2000. Vertebrate orthologues of the *Drosophila* region-specific patterning gene teashirt. Mech. Dev. 91, 445–448.
Caubit, X., Tiveron, M.C., Cremer, H., Fasano, L., 2005. Expression patterns of the three Teashirt-related genes define specific boundaries in the developing and postnatal mouse forebrain. J. Comp. Neurol. 486, 76–88.
Chisaka, O., Capecchi, M.R., 1991. Regionally restricted developmental defects resulting from targeted disruption of the mouse homeobox gene hox-1.5. Nature 350, 473–479.
Cody, J.D., Ghidoni, P.D., DuPont, B.R., Hale, D.E., Hilsenbeck, S.G., Stratton, R.F., Hoffman, D.S., Muller, S., Schaub, R.L., Leach, R.J., Kaye, C.I., 1999. Congenital anomalies and anthropometry of 42 individuals with deletions of chromosome 18q. Am. J. Med. Genet. 85, 455–462.
Core, N., Bel, S., Gaunt, S.J., Aurrand-Lions, M., Pearce, J., Fisher, A., Djabali, M., 1997. Altered cellular proliferation and mesoderm patterning in Polycomb-M33-deficient mice. Development 124, 721–729.
Cremers, C.W., Teunissen, E., Marres, E.H., 1988. Classification of congenital aural atresia and results of reconstructive surgery. Adv. Otorhinolaryngol. 40, 9–14.
de Zulueta, P., Alexandre, E., Jacq, B., Kerridge, S., 1994. Homeotic complex and teashirt genes co-operate to establish trunk segmental identities in *Drosophila*. Development 120, 2287–2296.
Dostal, A., Nemeckova, J., Gaillyova, R., Vranova, V., Zezulkova, D., Lejska, M., Slapak, I., Dostalova, Z., Kuglik, P., 2006. Identification of 2.3-Mb gene locus for congenital aural atresia in 18q22.3 deletion: a case report analyzed by comparative genomic hybridization. Otol. Neurotol. 27, 427–432.
Ducy, P., Zhang, R., Geoffroy, V., Ridall, A.L., Karsenty, G., 1997. Osf2/Cbfa1: a transcriptional activator of osteoblast differentiation. Cell 89, 747–754.
Erkner, A., Gallet, A., Angelats, C., Fasano, L., Kerridge, S., 1999. The role of Teashirt in proximal leg development in *Drosophila*: ectopic Teashirt expression reveals different cell behaviours in ventral and dorsal domains. Dev. Biol. 215, 221–232.
Fasano, L., Roder, L., Core, N., Alexandre, E., Vola, C., Jacq, B., Kerridge, S., 1991. The gene teashirt is required for the development of *Drosophila* embryonic trunk segments and encodes a protein with widely spaced zinc finger motifs. Cell 64, 63–79.
Gaunt, S.J., 1987. Homoeobox gene Hox-1.5 expression in mouse embryos: earliest detection by in situ hybridization is during gastrulation. Development 101, 51–60.
Gaunt, S.J., 1988. Mouse homeobox gene transcripts occupy different but overlapping domains in embryonic germ layers and organs: a comparison of Hox-3.1 and Hox-1.5. Development 103, 135–144.
Gaunt, S.J., Blum, M., De Robertis, E.M., 1993. Expression of the mouse goosecoid gene during mid-embryogenesis may mark mesenchymal cell lineages in the developing head, limbs and body wall. Development 117, 769–778.
Grigoriou, M., Tucker, A.S., Sharpe, P.T., Pachnis, V., 1998. Expression and regulation of Lhx6 and Lhx7, a novel subfamily of LIM homeodomain encoding genes, suggests a role in mammalian head development. Development 125, 2063–2074.
Hall, B.K., Miyake, T., 2000. All for one and one for all: condensations and the initiation of skeletal development. BioEssays 22, 138–147.
Henrique, D., Adam, J., Myat, A., Chitnis, A., Lewis, J., Ish-Horowicz, D., 1995. Expression of a Delta homologue in prospective neurons in the chick. Nature 375, 787–790.
Horan, G.S., Kovacs, E.N., Behringer, R.R., Featherstone, M.S., 1995. Mutations in paralogous Hox genes result in overlapping homeotic transformations of the axial skeleton: evidence for unique and redundant function. Dev. Biol. 169, 359–372.
Hunt, P., Gulisano, M., Cook, M., Sham, M.H., Faiella, A., Wilkinson, D., Boncinelli, E., Krumlauf, R., 1991. A distinct Hox code for the branchial region of the vertebrate head. Nature 353, 861–864.
Keppler-Noreuil, K.M., Carroll, A.J., Finley, S.C., Descartes, M., Cody, J.D., DuPont, B.R., Gay, C.T., Leach, R.J., 1998. Chromosome 18q paracentric inversion in a family with mental retardation and hearing loss. Am. J. Med. Genet. 76, 372–378.
Kline, A.D., White, M.E., Wapner, R., Rojas, K., Biesecker, L.G., Kamholz, J., Zackai, E.H., Muenke, M., Scott Jr., C.I., Overhauser, J., 1993. Molecular analysis of the 18q-syndrome—and correlation with phenotype. Am. J. Hum. Genet. 52, 895–906.
Le Mouellic, H., Lallemand, Y., Brulet, P., 1992. Homeosis in the mouse induced by a null mutation in the Hox-3.1 gene. Cell 69, 251–264.
Lettice, L., Hecksher-Sorensen, J., Hill, R., 2001. The role of Bapx1 (Nkx3.2) in the development and evolution of the axial skeleton. J. Anat. 199, 181–187.
Long, Q., Park, B.K., Ekker, M., 2001. Expression and regulation of mouse Mtsh1 during limb and branchial arch development. Dev. Dyn. 222, 308–312.
Mallo, M., 2003. Formation of the outer and middle ear, molecular mechanisms. Curr. Top. Dev. Biol. 57, 85–113.
Mallo, M., Gridley, T., 1996. Development of the mammalian ear: coordinate regulation of formation of the tympanic ring and the external acoustic meatus. Development 122, 173–179.
Mallo, M., Schrewe, H., Martin, J.F., Olson, E.N., Ohnemus, S., 2000. Assembling a functional tympanic membrane: signals from the external acoustic meatus coordinate development of the malleal manubrium. Development 127, 4127–4136.
Manfroid, I., Caubit, X., Kerridge, S., Fasano, L., 2004. Three putative murine Teashirt orthologues specify trunk structures in *Drosophila* in the same way as the *Drosophila teashirt* gene. Development 131, 1065–1073.
Mathies, L.D., Kerridge, S., Scott, M.P., 1994. Role of the teashirt gene in *Drosophila* midgut morphogenesis: secreted proteins mediate the action of homeotic genes. Development 120, 2799–2809.
McCormick, A., Core, N., Kerridge, S., Scott, M.P., 1995. Homeotic response elements are tightly linked to tissue-specific elements in a transcriptional enhancer of the teashirt gene. Development 121, 2799–2812.
McKnight, S.L., 1980. The nucleotide sequence and transcript map of the herpes simplex virus thymidine kinase gene. Nucleic Acids Res. 8, 5949–5964.
Morais da Silva, S., Hacker, A., Harley, V., Goodfellow, P., Swain, A., Lovell-Badge, R., 1996. Sox9 expression during gonadal development implies a conserved role for the gene in testis differentiation in mammals and birds. Nat. Genet. 14, 62–68.
Morasso, M.I., Markova, N.G., Sargent, T.D., 1996. Regulation of epidermal differentiation by a Distal-less homeodomain gene. J. Cell Biol. 135, 1879–1887.
Morita, H., Mazerbourg, S., Bouley, D.M., Luo, C.W., Kawamura, K., Kuwabara, Y., Baribault, H., Tian, H., Hsueh, A.J., 2004. Neonatal lethality of LGR5 null mice is associated with ankyloglossia and gastrointestinal distension. Mol. Cell. Biol. 24, 9736–9743.
Morsli, H., Choo, D., Ryan, A., Johnson, R., Wu, D.K., 1998. Development of the mouse inner ear and origin of its sensory organs. J. Neurosci. 18, 3327–3335.
Noden, D.M., Francis-West, P., 2006. The differentiation and morphogenesis of craniofacial muscles. Dev. Dyn. 235, 1194–1218.
Ott, T., Kaestner, K.H., Monaghan, A.P., Schutz, G., 1996. The mouse homolog of the region specific homeotic gene spalt of *Drosophila* is expressed in the developing nervous system and in mesoderm-derived structures. Mech. Dev. 56, 117–128.
Pan, D., Rubin, G.M., 1998. Targeted expression of teashirt induces ectopic eyes in *Drosophila*. Proc. Natl. Acad. Sci. U. S. A. 95, 15508–15512.
Parrish, M., Ott, T., Lance-Jones, C., Schuetz, G., Schwaeger-Nickolenko, A., Monaghan, A.P., 2004. Loss of the Sall3 gene leads to palate deficiency, abnormalities in cranial nerves, and perinatal lethality. Mol. Cell. Biol. 24, 7102–7112.
Peters, H., Neubuser, A., Kratochwil, K., Balling, R., 1998. Pax9-deficient mice

lack pharyngeal pouch derivatives and teeth and exhibit craniofacial and limb abnormalities. Genes Dev. 12, 2735–2747.

Qiu, M., Bulfone, A., Ghattas, I., Meneses, J.J., Christensen, L., Sharpe, P.T., Presley, R., Pedersen, R.A., Rubenstein, J.L., 1997. Role of the Dlx homeobox genes in proximodistal patterning of the branchial arches: mutations of Dlx-1, Dlx-2, and Dlx-1 and -2 alter morphogenesis of proximal skeletal and soft tissue structures derived from the first and second arches. Dev. Biol. 185, 165–184.

Rivera-Perez, J.A., Mallo, M., Gendron-Maguire, M., Gridley, T., Behringer, R.R., 1995. Goosecoid is not an essential component of the mouse gastrula organizer but is required for craniofacial and rib development. Development 121, 3005–3012.

Robert, B., Sassoon, D., Jacq, B., Gehring, W., Buckingham, M., 1989. Hox-7, a mouse homeobox gene with a novel pattern of expression during embryogenesis. EMBO J. 8, 91–100.

Roder, L., 1992. Vol. thesis. University of Aix-Marseille II, Marseille.

Roder, L., Vola, C., Kerridge, S., 1992. The role of the teashirt gene in trunk segmental identity in *Drosophila*. Development 115, 1017–1033.

Santagati, F., Rijli, F.M., 2003. Cranial neural crest and the building of the vertebrate head. Nat. Rev., Neurosci. 4, 806–818.

Satokata, I., Maas, R., 1994. Msx1 deficient mice exhibit cleft palate and abnormalities of craniofacial and tooth development. Nat. Genet. 6, 348–356.

Shamblott, M.J., Bugg, E.M., Lawler, A.M., Gearhart, J.D., 2002. Craniofacial abnormalities resulting from targeted disruption of the murine Sim2 gene. Dev. Dyn. 224, 373–380.

Singh, A., Kango-Singh, M., Sun, Y.H., 2002. Eye suppression, a novel function of teashirt, requires Wingless signaling. Development 129, 4271–4280.

Strathdee, G., Zackai, E.H., Shapiro, R., Kamholz, J., Overhauser, J., 1995. Analysis of clinical variation seen in patients with 18q terminal deletions. Am. J. Med. Genet. 59, 476–483.

ten Berge, D., Brouwer, A., Korving, J., Martin, J.F., Meijlink, F., 1998. Prx1 and Prx2 in skeletogenesis: roles in the craniofacial region, inner ear and limbs. Development 125, 3831–3842.

Tiveron, M.C., Hirsch, M.R., Brunet, J.F., 1996. The expression pattern of the transcription factor Phox2 delineates synaptic pathways of the autonomic nervous system. J. Neurosci. 16, 7649–7660.

Trainor, P.A., Tam, P.P., 1995. Cranial paraxial mesoderm and neural crest cells of the mouse embryo: co-distribution in the craniofacial mesenchyme but distinct segregation in branchial arches. Development 121, 2569–2582.

Tucker, A.S., Watson, R.P., Lettice, L.A., Yamada, G., Hill, R.E., 2004. Bapx1 regulates patterning in the middle ear: altered regulatory role in the transition from the proximal jaw during vertebrate evolution. Development 131, 1235–1245.

Tzahor, E., Kempf, H., Mootoosamy, R.C., Poon, A.C., Abzhanov, A., Tabin, C.J., Dietrich, S., Lassar, A.B., 2003. Antagonists of Wnt and BMP signaling promote the formation of vertebrate head muscle. Genes Dev. 17, 3087–3099.

Waltzer, L., Vandel, L., Bienz, M., 2001. Teashirt is required for transcriptional repression mediated by high Wingless levels. EMBO J. 20, 137–145.

Winograd, J., Reilly, M.P., Roe, R., Lutz, J., Laughner, E., Xu, X., Hu, L., Asakura, T., vander Kolk, C., Strandberg, J.D., Semenza, G.L., 1997. Perinatal lethality and multiple craniofacial malformations in MSX2 transgenic mice. Hum. Mol. Genet. 6, 369–379.

Yamada, G., Mansouri, A., Torres, M., Stuart, E.T., Blum, M., Schultz, M., De Robertis, E.M., Gruss, P., 1995. Targeted mutation of the murine goosecoid gene results in craniofacial defects and neonatal death. Development 121, 2917–2922.

Zhang, Z., Zhang, X., Avniel, W.A., Song, Y., Jones, S.M., Jones, T.A., Fermin, C., Chen, Y., 2003. Malleal processus brevis is dispensable for normal hearing in mice. Dev. Dyn. 227, 69–77.